Supplemental Information

CONTENTS

SUPPLEMENTARY METHODS

Mice and experimental procedure

All experiments with mice were performed according to protocols approved by the Institutional Animal Care and Use Committees of Children's Hospital Boston or Beth Israel Deaconess Medical Center. *Wt1*$^{GFPCre/+}$, *Wt1*$^{CreERT2/+}$, *Rosa26*$^{fsLz/+}$; *TNTCre*; *iTNT-Cre*; and *Rosa26*$^{mTmG/+}$ were described previously (1-5). Embryo gestational age was determined from timed matings, with the noon of the day of the vaginal plug defined as day 0.5. We administered tamoxifen (1 mg/10 g body weight) by gavage to pregnant mice at E10.5 to induce Cre. Matrigel plugs were injected into flanks of nude mice (Charles River) as described previously (6). For adult mice, 4 mg tamoxifen (Tam, Sigma) was administered by gavage to 6-9 week old mice twice weekly for 2-3 weeks.

One week after completion of Tam dosing, myocardial infarction (MI) was induced by ligation of left anterior descending coronary artery as previously described (7). Briefly, mice were anesthetized with isofluorane blended with oxygen (2-4% isofluorane for induction, 1-3% for maintenance). The chest were shaved and cleaned with alcohol. A suture was placed around the front upper incisors and pulled taut so that the neck was slightly extended. The tongue was retracted and held with forceps, and a 20-G catheter was inserted into the trachea. The catheter was then attached to the mouse ventilator via a Y-shaped connector. Ventilation was performed with a tidal volume of 200 µl and a respiratory rate of 133/min. 100% oxygen was provided to the inflow of the ventilator. Prior to the incision, 0.1 ml of 0.1% lidocaine was introduced under the skin. The chest cavity was opened by an incision of the left second intercostal space. Chest

retractor was applied to facilitate the view. The pericardial sac was opened. The left anterior descending artery was ligated using 7-0 silk suture. Lungs were slightly overinflated to assist in removal of air in the pleural cavity. The chest cavity, muscles, and skin are closed layer by layer. The duration of the whole procedure amounts to about 15-20 min. Postoperative analgesics (0.05-0.1 mg/kg Buprenorphine s.c.) were given every 8-12 h for 48 hours. The sham procedure included opening of the pericardium and was identical except that the coronary artery was not ligated. Survival rate one week after MI was 70-75%. MI size was determined by 2,3,5-Triphenyl Tetrazolium Chloride (TTC) assay (8).

To determine the effect of conditioned media on development of myocardial infarction, EPDC conditioned media or unconditioned control media were prepared and concentrated as described below and injected into four sites in the infarct border zone immediately after ligation of the left anterior descending coronary artery. MI experiments were performed and analyzed blinded to treatment group.

Canine heart injury model

All canine studies were performed in accordance with protocols approved by the BIDMC Institutional Animal Care and Use Committee. MI was produced in mongrel dogs weighing 25 to 30 kg by a 2-stage ligation of the left anterior descending coronary artery near its origin, as described previously (9). The chest was closed after the occlusion and the animals recovered from anesthesia. The animals were reanesthetized at the time of tissue harvesting. Hearts were quickly excised, washed in cold Tyrode's solution, sliced, stained in TTC for 1.5 hrs and fixed in 10% formalin for 30 minutes. Tissue was subsequently processed for immunohistochemistry.

Ad:Msln-Cre construction and ultrasound-guided injection

The human *Msln* promoter (1.85 kb) was PCR cloned and inserted into NotI and XbaI sites of pShuttle (Stratagene). Cre followed by a synthetic polyA sequence was inserted into XbaI and HindIII sites. The Msln-Cre construct was recombined with pAdEasy vector in bacteria, and

the resulting construct was transfected into 293 AD cells (Stratagene) to generate virus. Virus was purified by CsCl gradient centrifugation and titered using the AdEasy viral titer kit (Stratagene).

For ultrasound-guided myocardial injection of adenovirus (10), Rosa26^{mTmG} mice were anesthetized with isofluorane and placed on the heated operating stage of a Vevo 770 microinjection system (VisualSonics, Toronto, Canada). After depilation and sterile preparation of the chest wall, the heart was imaged using sterile ultrasound gel. We empirically determined the optimal injection points that permitted labeling of the territory supplied by left anterior descending coronary artery (11) while avoiding injury of the lung. The adenovirus (3.8×10^9 pfu/ml) was loaded into a syringe with a 1/2 inch 30G steel needle. The needle was advanced through the chest wall and into the heart so that the tip was judged to be at the LV myocardium. 100 µl was then injected. The entire procedure was performed with aseptic technique and the mouse was monitored with electrocardiography.

Immunohistochemistry

Immunostaining was performed as described previously (12). Embryos and adult hearts were collected in PBS on ice and then fixed in 4% PFA at 4°C for 2 hours to overnight. After washing in PBS, tissues were treated sequentially with 15% and 30% sucrose until tissue was fully penetrated. Then they were embeded in OCT and snap frozen. 6-10 µm cryosections were collected on positively charged slides. Tissues were blocked with PBS supplemented with 0.1% triton X-100 and 5% normal donkey serum for 1 hour at room temperature, followed by first antibody incubation at 4°C overnight. Antibody sources were listed in Supplemental Table 1. Signals were developed with Alexa or HRP-conjugated secondary antibodies (Invitrogen). To use the red channel in *Rosa26*$^{mTmG/+}$ samples, we bleached tissue sections with 100% methanol supplemented with 3% H_2O_2 on a fluorescent illuminator at 4°C overnight. The Images were acquired on a FV1000 confocal microscope (Olympus) or Eclipse 80i microscope (Nikon).

Spectral analyses were performed according to previously described protocols (13). Briefly, images were acquired using the lambda acquisition mode of the FV1000 confocal microscope (Olympus). GFP fluorescence was excited at 488 nm and fluorescent emission was recorded from 493 to 603 nm at 10 nm intervals. In each region of interest, the signal intensity average was then calculated each each different emission wavelength. Emission spectra were plotted as the ratio of the intensity at each wavelength to the maximum intensity. The characteristic GFP emission spectrum was distinct from autofluorescent emission spectra. The difference in shapes could be represented by the ratio of signal at a shoulder wavelength (eg 533 nm) to the peak wavelength (503 nm).

Primary cell isolation and culture

The apical regions of $Wt1^{CreERT2/+}$; $Rosa26^{mTmG/+}$ embryonic hearts were isolated by microdissection and dissociated to single cells by collagenase digestion as previously described (14). Tissue from 2-3 embryos was pooled into one sample. $Wt1^{CreERT2/+}$; $Rosa26^{mTmG/+}$ adult hearts were digested with collagenase IV. Single cell suspensions were FACS sorted into GFP^+ and GFP^- populations as described in the following section. For RNA, sorted cells were collected into Trizol (Invitrogen). For cell culture, sorted cells were collected into MSCGM (Mesenchymal Stem Cell Growth Medium, Lonza) with 20% FBS and cultured in MSCGM/10% FBS.

To prepare EPDC conditioned medium, EPDCs from a single heart were expanded and cultured to confluence in MSCGM (Lonza). Cells were then switched to EBM2 (Lonza) medium without serum for 24 hours. The supernatant was collected and filtered through 0.2 μm Nalgene filter, then concentrated using Amicon Ultra centrifugal filters (Regenerated cellulose, 3 kDa molecular weight cut off) to reduce the volume by 30-fold. For in vitro experiments, CM derived from different individual mice were kept separate, while they were pooled for in vivo experiments. To make highly concentrated medium for the corneal micropocket assay, we

pooled the concentrated CM from EPDCs from several different mice. The pooled CM was re-concentrated and then lyophilized. Concentrated conditioned media could be frozen and thawed once without loss of activity in in vitro assays. For hypoxia, cells were grown in a hypoxia chamber with 1% oxygen.

Cord blood endothelial cells were isolated as described previously (6). Bone marrow cells were flushed from the femurs and tibias of mice with ice-cold HBSS (15). Mouse bmMSCs were further purified by depletion of $CD45^+$ hematopoietic cells by magnetic cell sorting (Miltenyi Biotec) and cultured in MSCGM medium. Lung endothelial cell lines were generated as previously described (16).

FACS Analysis and Sorting

For FACS analsysis, dissociated cells were labeled with APC-conjugated antibodies (1:100) at 4°C for 20 minutes followed by 3 washes with PBS/1% BSA/0.2 mM EDTA and resuspended in 1% paraformaldehyde in PBS. If cells were sorted for isolation of viable GFP^+ and GFP^- populations, we resuspended dissociated cells in Hank's balanced salt solution. Flow cytometric analysis and isolation were performed using a Beckman Coulter MoFlo Legacy machine and Dako Summit software. For cell culture, all procedure and equipment were kept sterile.

MTT, Proliferation and Apoptosis Assays

Proliferation of endothelial cells treated with CM was measured by direct counting of endothelial cells or by MTT assay using Celltiter 96 Aqueous One solution (Promega). After adding the Celltiter 96 Aqueous One reagent into the cell culture medium, we incubated the plate at 37°C for 3-4 hours, and then recorded the absorbance at 490nm using a 96-well plate reader. Higher absorbance at 490nm was tightly correlated with higer cell number ($r = 0.993$). The MTT readout on the y-axis, labeled MTT assay A_{490}, thus reflects the relative number of cells from each well between groups of treatment. Direct evidence of proliferation was also provided by incorporation of BrdU (100 μM for 1 hour). After fixation, BrdU was detected by

treating cells with 2N HCl at 37°C for half an hour followed by staining with BrdU antibody as previously described (17). Apoptosis was detected with the In Situ Cell Death Detection Kit (TUNEL, Roche) and cleaved Caspase 3 antibody (Cell Signaling Technology).

To screen CM for active factors, neutralizing antibodies were diluted according to manufacturer protocols (R&D, Peprotech). Antibodies to factors were used at the following concentrations: 3 µg/ml FGF1 (R&D AF232), 100 µg/ml FGF2 (R&D AB-233-NA, Millipore 05-117), 10 µg/ml Osteopontin (R&D AF808), 60 µg/ml MCP1 (R&D AB-479-NA), 6 µg/ml SDF1 (R&D AF-310-NA), 30 µg/ml IGFBP2 (R&D AF797), 5 µg/ml IGFBP3 (R&D AF675), 10 µg/ml Jagged1 (R&D AF1277), 5 µg/ml VEGF (Peprotech 500-P131).

Gene expression analysis

RNA was extracted with Trizol according to manufacturer's protocol (Invitrogen) and converted the RNA to cDNA using Superscript III reverse transcriptase (Invitrogen). For quantitative PCR, we used SYBR Green qPCR master mix (Applied Biosystems) and amplified cDNA on an ABI 7500 Sequence Detector (Applied Biosystems). Primer sequences are provided in Supplemental Table 2.

We used Proteome Profiler Array system (R & D) to measure angiogenesis-related protein expression in CM according to manufacturer's protocol. To quantitatively measure protein level, we used VEGFA Elisa (R & D) and FGF2 Elisa (RayBiotech) according to the manufacturers' protocols.

In vitro tubule formation assay

The tubule formation assay was performed on matrigel (BD Biosciences), using 3-6 x 10^4 endothelial cells or EPDC for coculture in EBM2 medium. Matrigel was thawed overnight at 4°C. Prior to adding cells, 200 µl matrigel was added per well of a 24 well dish and allowed to gel at at 37°C for an hour (18).

Matrigel plug assay

The matrigel plug assay was used as in vivo angiogenesis model as described (6, 19). Briefly, a total of $2x10^6$ cells (equal number of endothelial cells and EPDCs) were resuspended in 200 µl phenol red-free, growth factor reduced Matrigel on ice (BD biosciences). The matrigel/ cell suspension was implanted into the flank of 6-8 week old nude mice (Charles River) by subcutaneous injection using a 25-gauge needle.

Cornea micropocket assay

The corneal micropocket assay was conducted as previously described to test the angiogenic effect of conditioned media (20). Briefly, 1.7×10^8 EPDC were cultured in serum free EBM2 for 24 hours. The conditioned media were concentrated using Amicon Ultra-15 filters (3000 MWCO). The CM was then lyophilized in a speedvac. The pellet was dissolved in sucrafate and hydron solution to make CM-loaded pellets. Unconditioned EBM2 media was used as a negative control. Pellets were implanted in the corneas of C57BL/6J mice. Blood vessel growth on the cornea was observed 6 days after pellet implantation using a slit lamp microscope.

Magnetic Resonance Imaging (MRI)

Heart function in vivo was measured by MRI. Mice were anaesthesized with 1-2% isofluorane/air mixture administered via a custom-designed nose cone. EKG, respiratory, and temperature probes were placed on the mouse, and the mouse was warmed on a heating pad. Images were acquired on a 4.7 T Bruker Biospec. A stack of short-axis slices covering the heart from the apex to the base and an orthogonal long-axis slice was acquired with an ECG-triggered and respiratory-gated Flash-CINE sequence with the following parameters: repetition time (TR) 25 msec, echo time (TE) 2.8 msec, 4 averages, slice thickness, 1 mm, matrix size 192 x 192 (2.56 x 2.56 cm), 5-7 frames per sequence (depending on RR interval). The resulting acquisition time per slice was approximately 5 min. Five short-axis slices were acquired from the

apex to the base to cover the left ventricle. Left ventricular (LV) ejection fraction was calculated as the difference in diastolic and systolic LV volumes, divided by the diastolic LV volume. MRI acquisition and analysis was performed blinded to treatment group.

Measurement of Cardiac Function

Hearts were isolated and perfused in Langendorff mode at 37°C and perfusion pressure of 80 mmHg as described previously (21). A water-filled balloon made of polyvinylchloride film was inserted in the LV and connected to a data acquisition system. After 30 min stabilization, the balloon volume (BV) which produced an LV end diastolic pressure (EDP) of 0 mmHg was determined. The BV was then increased in 2-5-µl increments until 40 µl. At each BV, the heart was allowed to stabilize for ~40 seconds, then indices of cardiac function were recorded. The BV was then adjusted to set EDP at ~10 mmHg and held constant. After the heart developed stable isovolumic contractions under these conditions, baseline function was recorded for 5 min. The heart was stimulated with 300 nM dobutamine by a side tubing attached to a digital console driver. After reaching steady state, cardiac function was measured for another 5 min. Function measurement and data analysis was performed blinded to the treatment groups. One CM sample was identified as an outlier by the extreme studentized deviate method and was removed from the analysis.

Statistical analyses

Unless otherwise noted, we evaluated statistical significance using Student's *t*-test. We considered $P < 0.05$ to be significant. Values were reported and displayed as mean ± standard error of the mean. In box and whisker plots, box and bar indicate 25, 50, and 75 percentiles, and whiskers indicate extreme values.

Supplemental References

1. Zhou, B., Ma, Q., Rajagopal, S., Wu, S.M., Domian, I., Rivera-Feliciano, J., Jiang, D., von Gise, A., Ikeda, S., Chien, K.R., and Pu, W.T. 2008. Epicardial progenitors contribute to the cardiomyocyte lineage in the developing heart. *Nature.* **454**:109-113.
2. Muzumdar, M.D., Tasic, B., Miyamichi, K., Li, L., and Luo, L. 2007. A global double-fluorescent Cre reporter mouse. *Genesis.* **45**:593-605.
3. Jiao, K., Kulessa, H., Tompkins, K., Zhou, Y., Batts, L., Baldwin, H.S., and Hogan, B.L. 2003. An essential role of Bmp4 in the atrioventricular septation of the mouse heart. *Genes Dev.* **17**:2362-2367.
4. Soriano, P. 1999. Generalized lacZ expression with the ROSA26 Cre reporter strain. *Nat Genet.* **21**:70-71.
5. Wu, B., Zhou, B., Wang, Y., Cheng, H.L., Hang, C.T., Pu, W.T., Chang, C.P., and Zhou, B. 2009. Inducible cardiomyocyte-specific gene disruption directed by the rat Tnnt2 promoter in the mouse. *Genesis.*
6. Melero-Martin, J.M., De Obaldia, M.E., Kang, S.Y., Khan, Z.A., Yuan, L., Oettgen, P., and Bischoff, J. 2008. Engineering robust and functional vascular networks in vivo with human adult and cord blood-derived progenitor cells. *Circ Res.* **103**:194-202.
7. Tarnavski, O., McMullen, J.R., Schinke, M., Nie, Q., Kong, S., and Izumo, S. 2004. Mouse cardiac surgery: comprehensive techniques for the generation of mouse models of human diseases and their application for genomic studies. *Physiol Genomics.* **16**:349-360.
8. Hutter, J.J., Mestril, R., Tam, E.K., Sievers, R.E., Dillmann, W.H., and Wolfe, C.L. 1996. Overexpression of heat shock protein 72 in transgenic mice decreases infarct size in vivo. *Circulation.* **94**:1408-1411.

9. Ursell, P.C., Gardner, P.I., Albala, A., Fenoglio, J.J.J., and Wit, A.L. 1985. Structural and electrophysiological changes in the epicardial border zone of canine myocardial infarcts during infarct healing. *Circ Res.* **56**:436-451.

10. Ikeda, S., He, A., Kong, S.W., Lu, J., Bejar, R., Bodyak, N., Lee, K.H., Ma, Q., Kang, P.M., Golub, T.R., and Pu, W.T. 2009. microRNA-1 negatively regulates expression of the hypertrophy-associated genes calmodulin and Mef2a. *Mol Cell Biol.*

11. Lang, R.M., Bierig, M., Devereux, R.B., Flachskampf, F.A., Foster, E., Pellikka, P.A., Picard, M.H., Roman, M.J., Seward, J., Shanewise, J.S., Solomon, S.D., Spencer, K.T., Sutton, M.S., and Stewart, W.J. 2005. Recommendations for chamber quantification: a report from the American Society of Echocardiography's Guidelines and Standards Committee and the Chamber Quantification Writing Group, developed in conjunction with the European Association of Echocardiography, a branch of the European Society of Cardiology. *J Am Soc Echocardiogr.* **18**:1440-1463.

12. Zhou, B., Bi, Y.Y., Han, Z.B., Ren, H., Fang, Z.H., Yu, X.F., Poon, M.C., and Han, Z.C. 2006. G-CSF-mobilized peripheral blood mononuclear cells from diabetic patients augment neovascularization in ischemic limbs but with impaired capability. *J Thromb Haemost.* **4**:993-1002.

13. D'Alessandro, D.A., Kajstura, J., Hosoda, T., Gatti, A., Bello, R., Mosna, F., Bardelli, S., Zheng, H., D'Amario, D., Padin-Iruegas, M.E., Carvalho, A.B., Rota, M., Zembala, M.O., Stern, D., Rimoldi, O., Urbanek, K., Michler, R.E., Leri, A., and Anversa, P. 2009. Progenitor Cells From the Explanted Heart Generate Immunocompatible Myocardium Within the Transplanted Donor Heart. *Circ Res.* **105**:1128-1140.

14. Zhou, B., von Gise, A., Ma, Q., Hu, Y.W., and Pu, W.T. 2010. Genetic fate mapping demonstrates contribution of epicardium-derived cells to the annulus fibrosis of the

mammalian heart. *Dev Biol.* **338**:251-261.

15. Soleimani, M., and Nadri, S. 2009. A protocol for isolation and culture of mesenchymal stem cells from mouse bone marrow. *Nat Protoc.* **4**:102-106.
16. Wang, L., Fuster, M., Sriramarao, P., and Esko, J.D. 2005. Endothelial heparan sulfate deficiency impairs L-selectin- and chemokine-mediated neutrophil trafficking during inflammatory responses. *Nat Immunol.* **6**:902-910.
17. Bisping, E., Ikeda, S., Kong, S.W., Tarnavski, O., Bodyak, N., McMullen, J.R., Rajagopal, S., Son, J.K., Ma, Q., Springer, Z., Kang, P.M., Izumo, S., and Pu, W.T. 2006. Gata4 is required for maintenance of postnatal cardiac function and protection from pressure overload-induced heart failure. *Proc Natl Acad Sci U S A.* **103**:14471-14476.
18. Zhou, B., Ma, Q., Kong, S.W., Hu, Y., Campbell, P.H., McGowan, F.X., Ackerman, K.G., Wu, B., Zhou, B., Tevosian, S.G., and Pu, W.T. 2009. Fog2 is critical for cardiac function and maintenance of coronary vasculature in the adult mouse heart. *J Clin Invest.*
19. Melero-Martin, J.M., Khan, Z.A., Picard, A., Wu, X., Paruchuri, S., and Bischoff, J. 2007. In vivo vasculogenic potential of human blood-derived endothelial progenitor cells. *Blood.* **109**:4761-4768.
20. Fernandez, C.A., Butterfield, C., Jackson, G., and Moses, M.A. 2003. Structural and functional uncoupling of the enzymatic and angiogenic inhibitory activities of tissue inhibitor of metalloproteinase-2 (TIMP-2): loop 6 is a novel angiogenesis inhibitor. *J Biol Chem.* **278**:40989-40995.
21. He, H., Javadpour, M.M., Latif, F., Tardiff, J.C., and Ingwall, J.S. 2007. R-92L and R-92W mutations in cardiac troponin T lead to distinct energetic phenotypes in intact mouse hearts. *Biophys J.* **93**:1834-1844.

Supplementary Table 1. Antibodies profile

Name	*Company*
WT1	Santa Cruz Biotechnology
GFP	Invitrogen
GFP	Abcam
GFP	Rockland
β-galatosidase	MP biomedicals
Cre recombinase	Covance
Cardiac Troponin T	Lab Vision
Sarcomeric a-Actinin	Sigma
BRDU	Sigma
GATA4	Santa Cruz Biotechnology
Smooth Muscle Myosin Heavy Chain	Biomedical Technology
Smooth muscle actin alpha	Sigma
Smooth muscle 22 alpha	Abcam
Estrogen receptor	Abcam
TBX18	Santa Cruz Biotechnology
GATA5	Sigma
Phospho-Histone 3	Millipore
PECAM	BD Biosciences
PECAM	Dako
VEGFR2	BD Biosciences
BS-1 Lectin, Griffonial Simplicifolia Lectin I	Vector Lab
Anti BS-1 lectin	Vector Lab
Fibronectin	Sigma
Desmin	Biomeda
Desmin	R & D
Collagen III	Southernbiotech
FSP1	Dako
Procollagen I	Santa Cruz Biotechnology
RFP	Rockland
UEA-I, Ulex Europaeus Agglutinin I	Vector Lab
Anti UEA-I	Vector Lab
Calponin	Abcam
NG2, chondriotin sulfate proteoglycan	Millipore
FGF2	R & D
VEGFA	Millipore
RALDH2	Sigma
pSmad2	Cell Signaling Technology
pSmad1/5/8	Santa Cruz Biotechnology
Slug	Cell Signaling Technology
Snail	Sigma

Epicardin	Abcam
VE-Cadherin	BD Biosciences
vWF	Dako
SPP-1	R & D
MCP1	R & D
SDF1	R & D
IGFBP3	R & D
Jagged1	R & D
FGF1	R & D
VEGF	Peprotech
CD90	eBiosciences
CD140	eBiosciences
CD45	eBiosciences
CD31	eBiosciences
CD29	eBiosciences
cleaved Caspase-3	Cell Signaling Technology
Alexa-488,555, 647	Invitrogen
Biotin-labeled 2nd Ab	Jackson Immunoresearch
HRP-labeled 2nd Ab	Jackson Immunoresearch
Immpress IgG polymer Ab	Vector Lab
SuperPicture rabbit and mouse polyHRP	Invitrogen
Elite ABC kit	Vector Lab
M.O.M. kit	Vector Lab
DAPI	Sigma

Supplementary Table 2

GENES	Forward	Backward
Gapdh	TTGTCTCCTGCGACTTCAAC	GTCATACCAGGAAATGAGCTTG
Cre	GCTCCTGTCTGTGTGCAGAT	GGGAACCATTTCCTGTTGTT
Wt1	AGACACACAGGTGTGAAACCA	ATGAGTCCTGGTGTGGGTCT
Wt1	GCCTTCACCTTGCACTTCTC	GACCGTGCTGTATCCTTGGT
Raldh2	TGGCAGAACTCAGAGAGTGG	CCACCTTGTCTGCTTCTTGA
Esr1	TCCTGGACAGGAATCAAGGT	AATGATGGATTTGAGGCACA
Msln	TGGACAAGACCTACCCACAA	TGGTGAGGTCACATTCCACT
Tbx18	AACAGAATGGGTTTGGAAGC	ACTTGTGTTGCCTTGCTTTG
Vegfa	GAGGATGTCCTCACTCGGAT	TCTCAGACCACACTGAAGCC
Vegfb	AGCCACCAGAAGAAAGTGGT	GCTGGGCACTAGTTGTTTGA
Vegfc	CCCAAACCAGTCACAATCAG	GGTAATGTTGCTGGCAGAGA
Fgf1	AGCTTTCTCCCAAGAGACCA	TCATGGCGTTTGTGTCCTAT
Fgf2	GCTGCTGGCTTCTAAGTGTG	TACTGCCCAGTTCGTTTCAG
Fgf9	GCGGTGGGTTCTTATTGATT	AAATTGGCAAGTCCTCATCC
Pdgfa	GCTGCACTGGCTGTTGTAA	ACTTTGGCCACCTTGACACT
Pdgfb	AGCTCCAGATGCAAAGGACT	CTGCACACTTGTTCCAGGTT
Pdgfc	AATTGTGCCTGTTGTCTCCA	TCAACTGAAGGACCTCATGG
Pdgfd	TGGCAAGATGATCTGGAGAA	AGAGTGATTCCTGGGAGTGC
Adamts1	CCCAAGGTTGTAGATGGCA	CCACAAACGCCACACTTATC
Tgfb2	AGCGCTACATCGATAGCAAG	TCCTGTCTTTGTGGTGAAGC
Jag1	CAGCGAATTGAGGAATTTGA	CTTGACAGGGTTCCCATCAT
Hgf	TTTCCAGCCAGAAACAAAGA	TCGCCTCTCTCATGAACATC
Sdf1	TATAGACGGTGGCTTTGCAG	TTGACTCAGGACAAGGCATC
Mcp1	GAAGGAATGGGTCCAGACAT	ACGGGTCAACTTCACATTCA
IL-6	AGTCCGGAGAGGAGACTTCA	ATTTCCACGATTTCCCAGAG
Igfbp3	AACCTGCTCCAGGAAACATC	ACAACCTGGCTTTCCACACT
Igfbp4	CGAAGCCATCCAGGAAAG	TGAAGCTGTTGTTGGGATGT
Igfbp5	GCAGGGAACCTGGAGAATAA	GATGTTCCCAAGCCTTGTCT
Igfbp6	GCTCCAGACTGAGGTCTTCC	GGAACGACACTGCTGCTTT
Myh6	ACATGAAGGAGGAGTTTGGG	GCACTTGGAGCTGTAGGTCA
TNNT2	CATCGACCACCTGAATGAAG	TTTCGCAGAACGTTGATTTC
Slug	CACATTCGAACCCACACATT	TATTGCAGTGAGGGCAAGAG
Snail	CGTGTGTGGAGTTCACCTTC	GGAGAGAGTCCCAGATGAGG
Smad	CCAAGCCAGGGACAAATTAT	TGATGAAAGCCCACTTCAGA
Twist	CGGACAAGCTGAGCAAGAT	GGACCTGGTACAGGAAGTCG
Postn	GACTGCTTCAGGGAGACACA	TGATCGTCTTCTAGGCCCTT
Col1a1	GGAAGAGCGGAGAGTACTGG	TTGCAGTAGACCTTGATGGC
Vim	GACATTGAGATCGCCACCTA	GGCAGAGAAATCCTGCTCTC
DDR2	CTGTGGGAGACCTTCACCTT	TAGATCTGCCTCCCTTGGTC
Tnc	CAGACTCAGCCATCACCAAC	CAGTTAACGCCCTGACTGTG
Fn1	ATCCAGGACGGGTCTGAG	CAGGAGCTCTAGGATTCGGA
Vegfa	GTCGGAGAGCAACGTCACTA	TCTCCTATGTGCTGGCTTTG

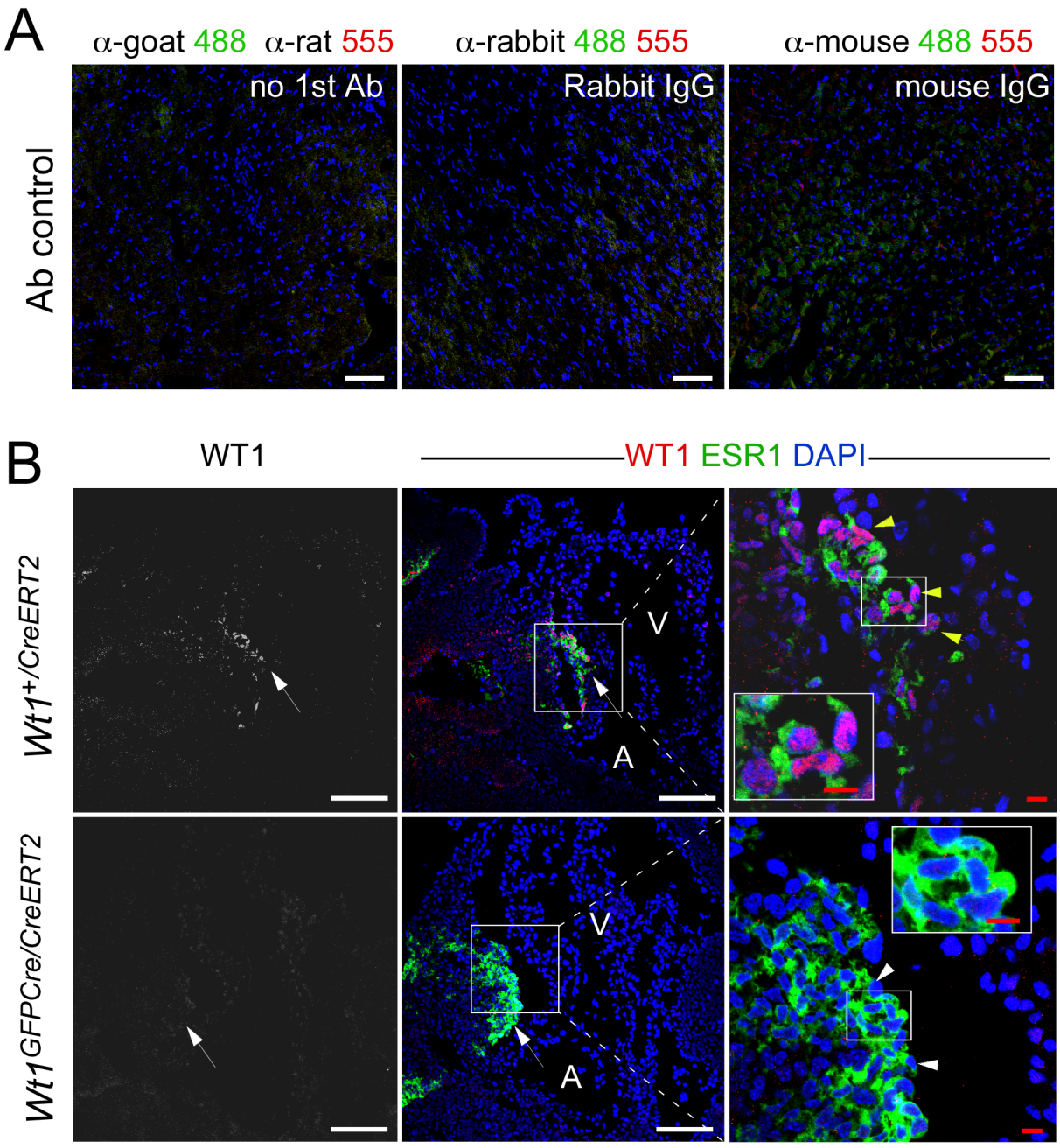

Supplemental Figure 1

Staining controls and WT1 expression in embryonic heart. (**A**) Negative control staining of heart sections using the indicated non-immune IgGs and 2nd antibodies conjugated with Alexa 488 and 555. (**B**) WT1 staining of sagittal sections of *Wt1* knockout (*Wt1*$^{GFPCre/CreERT2}$) and control (*Wt1*$^{CreERT2/+}$) E9.5 embryos to demonstrate staining specificity. In control, proepicardium (arrow) stained with both WT1 and ESR1, which stains CreERT2 expressed from Wt1^{CreERT2}. In *Wt1* knockout, ESR1 continues to mark PE, but WT1 immunoreactivity was no longer detected. A, atrium; V, ventricle. White bar = 100 μm; red bar = 10 μm.

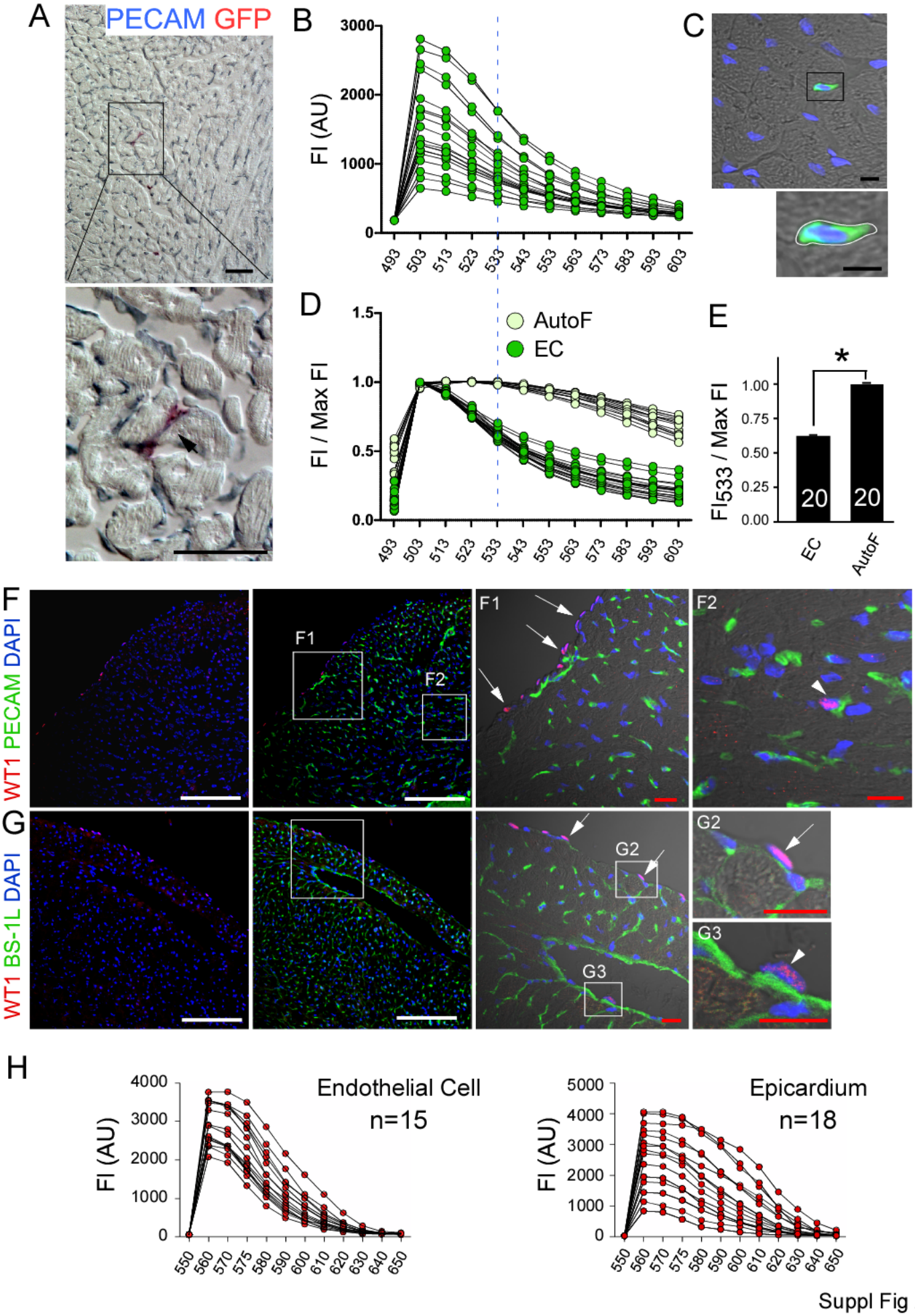
A
PECAM GFP
B
FI (AU)
3000
2000
1000
0
493 503 513 523 533 543 553 563 573 583 593 603
C
D
FI / Max FI
1.5
1.0
0.5
0.0
AutoF
EC
493 503 513 523 533 543 553 563 573 583 593 603
E
FI533 / Max FI
1.00
0.75
0.50
0.25
0.00
*
20
20
EC
AutoF
F
WT1 PECAM DAPI
F1
F2
G
WT1 BS-1L DAPI
G2
G3
H
Endothelial Cell
n=15
Epicardium
n=18
FI (AU)
4000
3000
2000
1000
0
5000
550 560 570 575 580 590 600 610 620 630 640 650

Suppl Fig 2

Supplemental Figure 2

Endogenous WT1 expression in adult heart. (**A**) Rare endothelial cells within $Wt1^{CreERT2/+}$; $Rosa26^{mTmG/+}$ myocardium treated with Tam in adulthood were labeled by GFP. However, this was likely due to expression of $Wt1^{CreERT2}$ within rare endothelial cells rather than differentiation of EPDCs into endothelial cells. Bar = 100 μm. (**B-C**) The emission spectrum of GFP^+ endothelial cells within myocardium was characteristic of GFP and not of autofluorescence, indicating *bona fide* GFP expression. The images show a representative GFP^+ *Wt1*-derived cell, with the white line demarcating the region of interest for emission spectrum acquisition. Bar = 10 μm; n = 20. FI, fluorescent intensity. AU, arbitrary units. (**D-E**) Normalization to maximum fluorescence intensity highlighted differences between true GFP signal and autofluorescence. At off-peak wavelengths (e.g. 533 nm), autofluorescent signals had higher normalized intensity compared to true GFP peaks. Normalized intensity of GFP^+ endothelial cells was consistent with true GFP signal, compared to autofluorescent cardiomyocytes (AutoF). Values are mean ± s.e.m. n = 14 - 20. $*P < 0.01$. (**F-G**) WT1 was expressed in epicardium (white arrows), where it was not colocalized with endothelial cell markers PECAM or BS-1 lectin. WT1 was also detected in rare endothelial cells within myocardium (white arrowheads). White bar = 200 μm; red bar = 20 μm. (**H**) Spectral analysis of $WT1^+$ endothelial cells and $WT1^+$ epicardial cells showed that they exhibit similar fluorescence intensity patterns. This confirmed that $WT1^+$ staining in rare endothelial cells was not an artifact caused by autofluorescence.

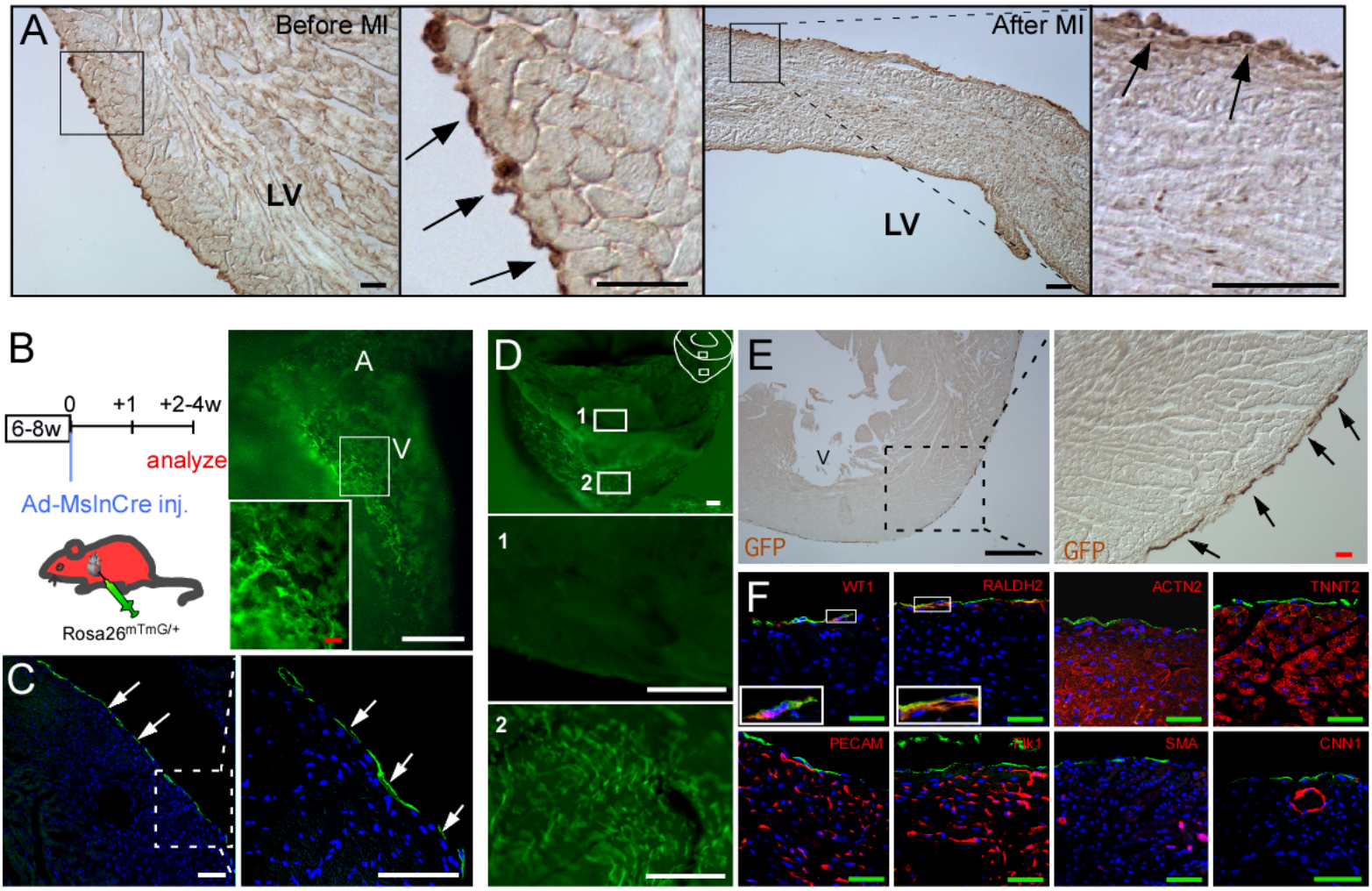

Supplemental Figure 3

MsIn-Cre virus injection and fate map of epicardial cells in normal heart. (**A**) Expression of MSLN in adult heart (black arrows). (**B-C**) Ultrasound-guided injection of Ad:MsIn-Cre into adult Rosa26$^{mTmG/+}$ heart labeled a subset of epicardium with GFP. Whole mount and sections 4 days post injection showed specific labeling of epicardium (white arrows). (**D-F**) Representative whole mount and section images show GFP distribution 4 weeks after virus injection. D shows whole mount fluorescence of apical portion of heart with illustrative diagram. Inserts d1 and d2 indicate myocardial and epicardial areas, respectively. E-F. Myocardial section stained for GFP. GFP was confined to the epicardial region (black arrows, E) in cells that expressed epicardial (WT1, RALDH2) but not cardiomyocyte (ACTN2, TNNT2) or vascular cell (PECAM, Flk1, SMA, CNN1) markers (E-F). A, atrium; V. ventricle. White or black bar = 200 μm; red bar = 20 μm, green bar = 100 μm.

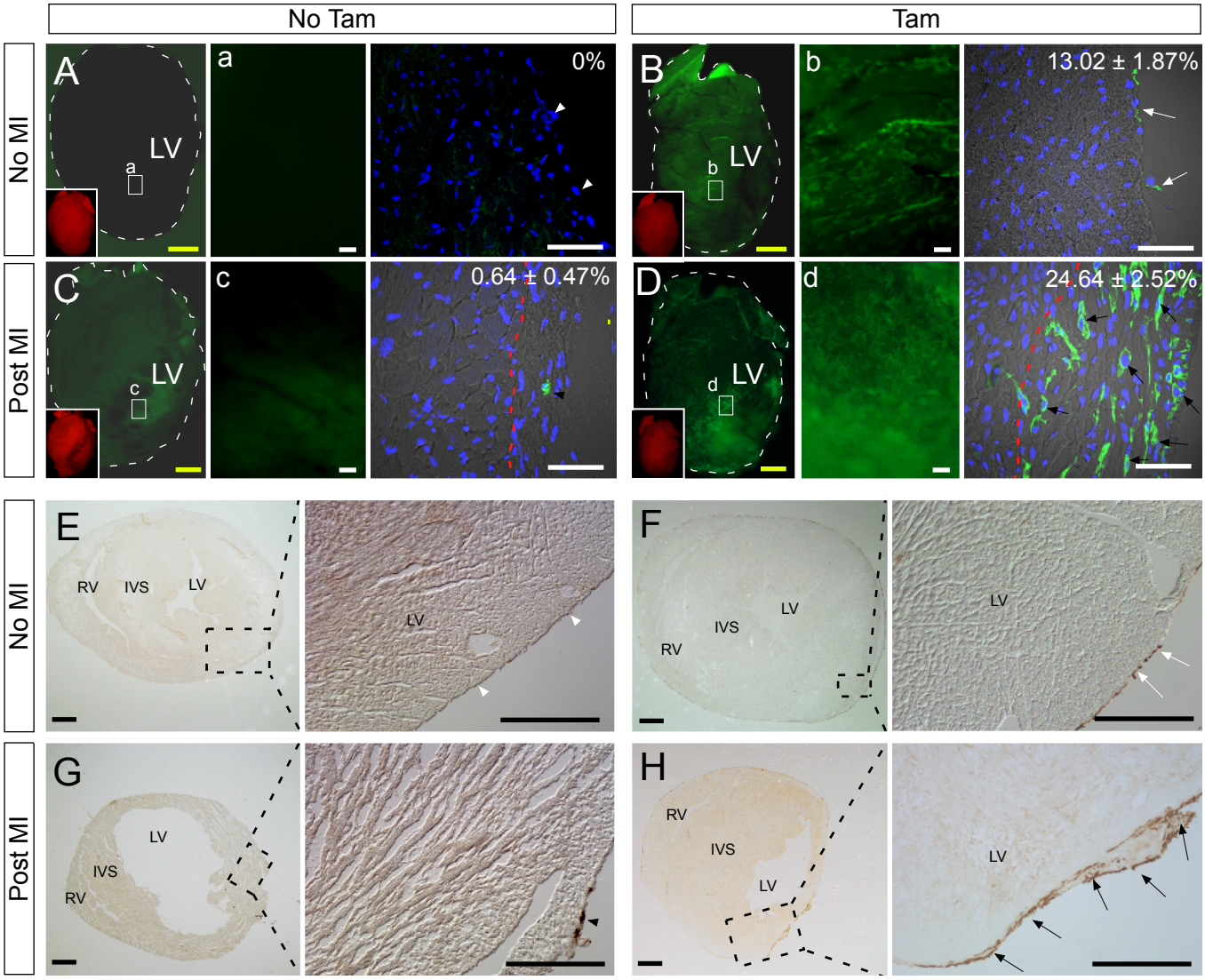

Supplemental Figure 4

Control experiments to validate Tam-induced Cre labeling and FACS sorting of EPDCs using *Wt1*$^{CreERT2/+}$;*Rosa26*$^{mTmG/+}$ mice. Wholemount and sections of hearts under four different conditions. Inserts on the bottom left (A-D) are wholemount figure of hearts in red channel. Dotted white lines indicate the outlines of the hearts in green channel. Tam^{-}/MI^{-} hearts exhibited no GFP expression in the epicardium (percentage of GFP+ cells in epicardium layer DAPI+ cells: 0%, white arrowheads, A, E). Tam^{+}/MI^{-} hearts showed some patches of GFP+ cells in the epicardium (13.02 ± 1.87%, n = 4, white arrows; B, F). Tam^{+}/MI^{+} hearts showed strong GFP label largely confined to epicardium (24.64 ± 1.04%, n = 7, black arrows; D, H). In Tam^{-}/MI^{+} hearts, no or very few GFP+ cells were detected in the epicardium layer (0.64 ± 0.47%, n = 5, black arrowhead; C, G), indicating relatively tight regulation of CreERT2 under stress conditions of MI. Yellow bar = 1 mm, white bar = 50 μm, black bar = 200 μm. LV, left ventricle; RV, right ventricle; IVS, interventricular septum.

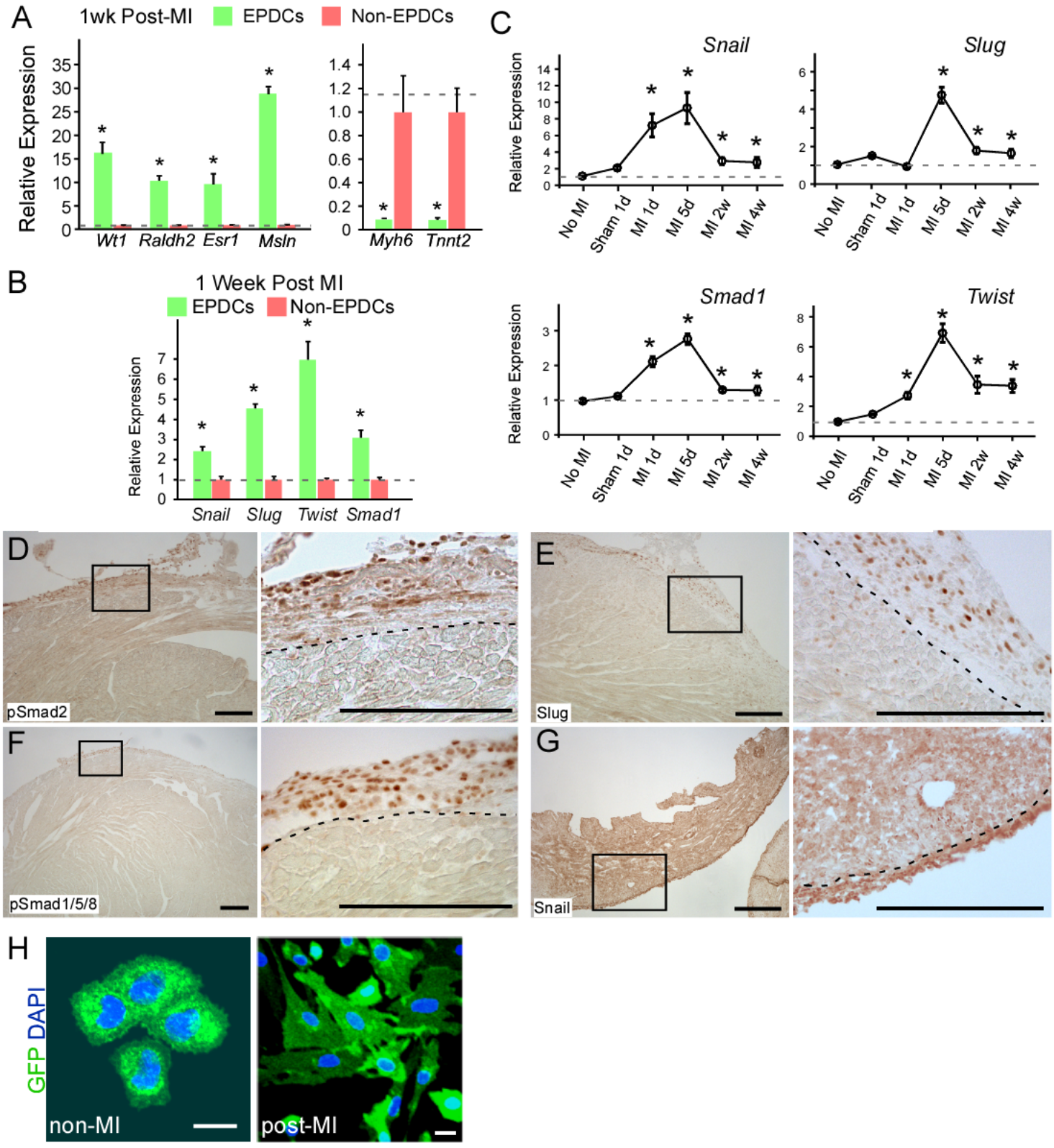

Supplemental Figure 5

Reactivation of Epicardial EMT after MI. (**A**) qRTPCR of FACS-purified EPDCs demonstrated strong enrichment of epicardial genes in EPDCs and myocardial genes in non-EPDCs, indicating effective sorting. (**B**) Enriched expression of EMT regulatory transcripts in FACS-purified EPDCs one week post-MI. n=3-6. (**C**) qRT-PCR of heart samples demonstrated dynamic expression of transcripts encoding EMT regulators after MI. (**D-G**) Immunohistochemistry showing upregulation of EMT regulatory proteins confined to epicardium one week after MI. pSMAD2 was strongly expressed and localized to the nucleus in the epicardial region (D). Strong, nuclear localized pSMAD1/5/8 immunoreactivity was also detected in the epicardial region (F). SLUG (E) and SNAIL (G) were also upregulated in the epicardium. Bar = 200 μm. Dotted line indicates border between epicardial region and myocardium. (**H**) Primary cultured (P0) EPDCs had epithelial morphology without MI and mesenchymal morphology post-MI. Bar = 10 μm.

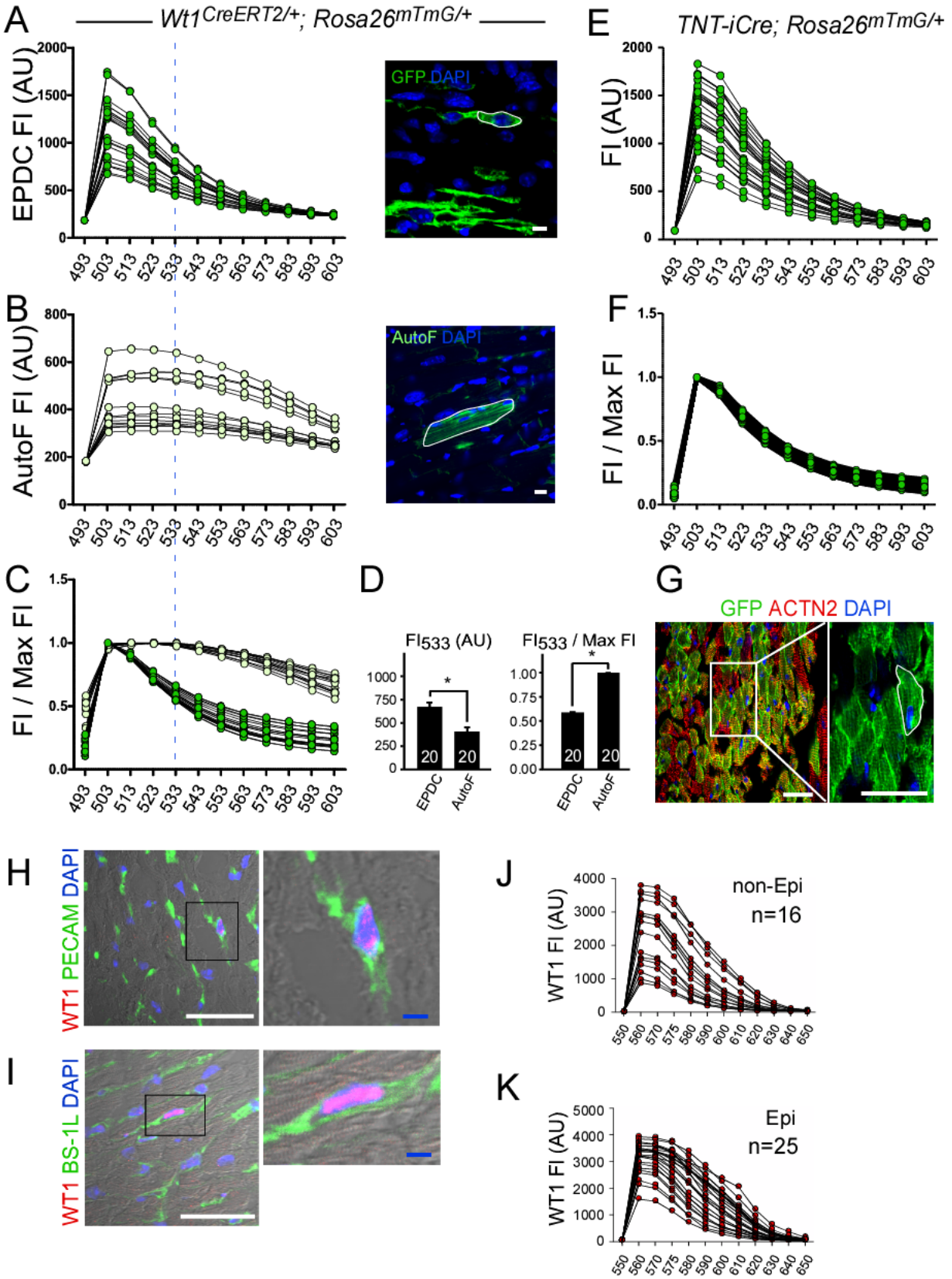
A
Wt1CreERT2/+; Rosa26mTmG/+
EPDC FI (AU)
GFP DAPI
E
TNT-iCre; Rosa26mTmG/+
FI (AU)
B
AutoF FI (AU)
AutoF DAPI
F
FI / Max FI
C
FI / Max FI
D
FI533 (AU)
FI533 / Max FI
EPDC
AutoF
G
GFP ACTN2 DAPI
H
WT1 PECAM DAPI
I
WT1 BS-1L DAPI
J
non-Epi
n=16
WT1 FI (AU)
K
Epi
n=25
WT1 FI (AU)

Suppl Fig 6

Supplemental Figure 6

Autofluorescence of cardiomyocytes and WT1 expression in endothelial cells after MI. (**A**) Emission spectral analysis of *bona fide* GFP-expressing cells in the epicardial region. Fluorescence intensity (FI) is plotted versus emission wavelength. A representative image shows GFP-expressing EPDCs, with one outlined in white for spectral analysis. Bar = 10 μm; n = 20. (**B**) Emission spectral analysis of weak green signals within morphological cardiomyocytes. Note the emission spectrum is different from *bona fide* GFP signal in (A). The representative image shows an autofluorescent cell outlined in white for spectral analysis. Bar = 10 μm; n = 14. (**C-D**) Emission spectra normalized to maximal fluorescent intensity clearly distinguishes true GFP signal from autofluorescent signal. The fluorescence intensity at 533 nm (dotted blue line) showed a significant difference in both FI_{553} and FI_{553}/ Max FI between EPDCs and autofluorescenced cardiomyocytes (AutoF) groups. Values are means ± s.e.m. (n = 14 - 20). *P < 0.01. (**E-G**) To provide a cardiomyocyte-specific GFP positive control, we activated GFP expression in cardiomyocytes using a dox-inducible Cre (TNT-iCre), activated in adult mice by treatment with dox for two weeks. The GFP reporter could be easily detected within cardiomyocytes marked with ACTN2. Emission spectral analysis showed that FI and FI / Max FI spectra were similar to that of EPDC, but distinct from that of autofluorescent cardiomyocytes. Comparison of fluorescent intensity at 533 nm showed a significant difference in FI_{533} and FI_{533} / Max FI between real GFP^+ cardiomyocytes and autofluorescent cardiomyocytes (data not shown). Bar = 50 μm; n = 20. (**H-I**) WT1 could also be detected in coronary endothelial cells, marked by PECAM or BS-1 lectin, in the injured heart after myocardial infarction. White bar = 50 μm; blue bar = 10 μm. **(J-K)** Spectral analysis revealed that endogenous WT1 in endothelial cells exhibited a fluorescence intensity (FI) pattern consistent with true fluorophore signal rather than autofluorescence.

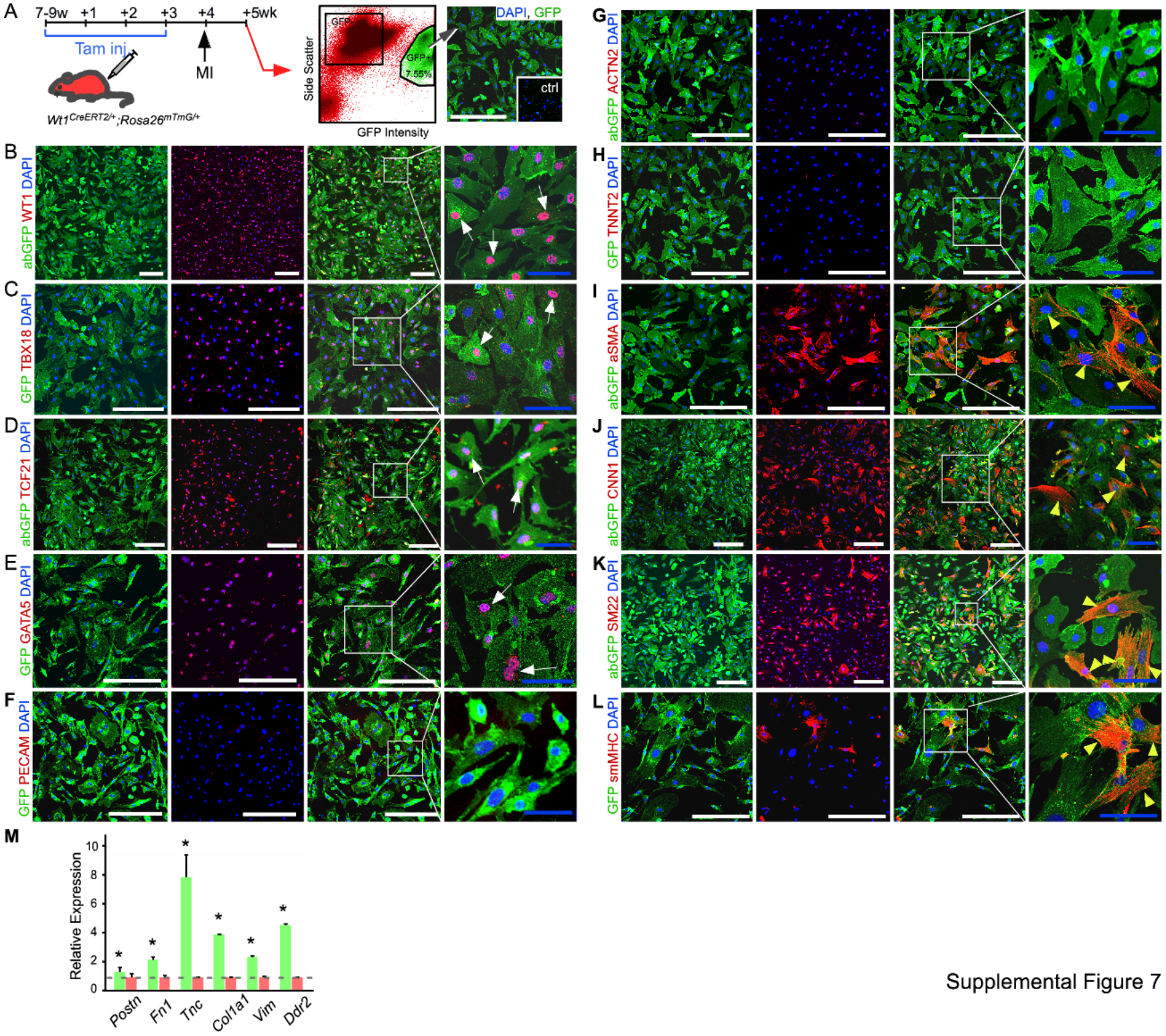

Supplemental Figure 7

Supplemental Figure 7 ***Post-MI EPDC expression of lineage markers.*** (**A**) Experimental outline. Tam treatment to label epicardial cells was followed by MI and then FACS purification of GFP^+ cells. The cells were plated on slides and transiently cultured, GFP^+ sorted cells showed strong green fluorescence without antibody staining, while there was no detectable signal in GFP^- cells (Ctrl, insert). (**B-E**) Epicardial markers WT1, TBX18, Epicardin (POD1), and GATA5 were expressed in most of EPDCs with hetergenous strength of expression (white arrows). (**F**) EDPCs did not express endothelial cell marker PECAM. (**G-H**) EPDCs did not express cardiomyocyte markers ACTN2 or TNNT2. (**I-L**) EPDCs expressed markers of mesenchymal cells (fibroblasts, myofibroblasts, and smooth muscle cells) smooth muscle actin (aSMA), smooth muscle myosin heavy chain (smMHC), SM22 alpha, Calponin (CNN1) (yellow arrowheads). White bar = 200 μm; blue bar = 50 μm. abGFP indicates GFP antibody staining, while GFP indicates endogenous GFP fluorescence.

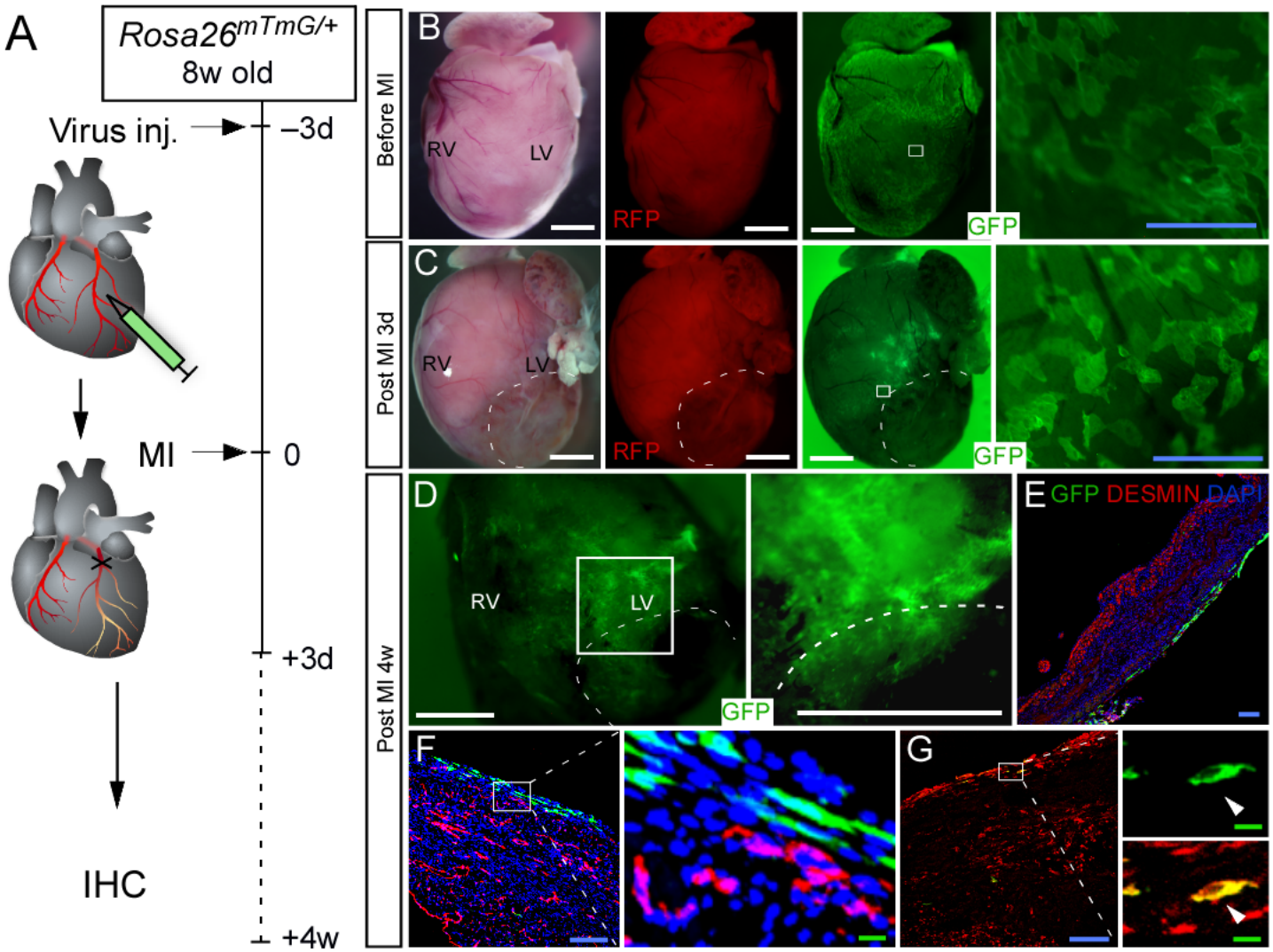

Supplemental Figure 8

Analysis of post-MI epicardial cell fate by Ad:Msln-Cre labeling. (**A**) Schematic showing the experimental outline. Ad:Msln-Cre virus was injected into hearts of *Rosa26*$^{mTmG/+}$ mice. Mice then underwent MI operation. Hearts were analyzed by immunohistochemistry (IHC) between 3d - 4w after MI. **(B)** Representative wholemount figure of Msln-Cre labeled cells after virus injection showing GFP and RFP fluorescence without antibody staining. LV, left ventricle; RV, right ventricle. (**C**) Wholemount figure of 3 days post MI heart. Dotted line indicates the infarcted area. (**D**) Wholemount figure of GFP-labeled hearts at 4 weeks after MI. Dotted line indicates the infarcted area. (**E**) GFP-labeled cells (green) were within the epicardial region, and few were within myocardium (red). (**F**) Msln-Cre marked cells (GFP^{+}) did not differentiate into PECAM^{+} endothelial cells (red). (**G**) Msln-Cre labeled cells (GFP^{+}) expressed FSP1^{+} fibroblast marker (white arrowhead). White bar = 2.0 mm; blue bar = 200 μm; green bar = 20 μm.

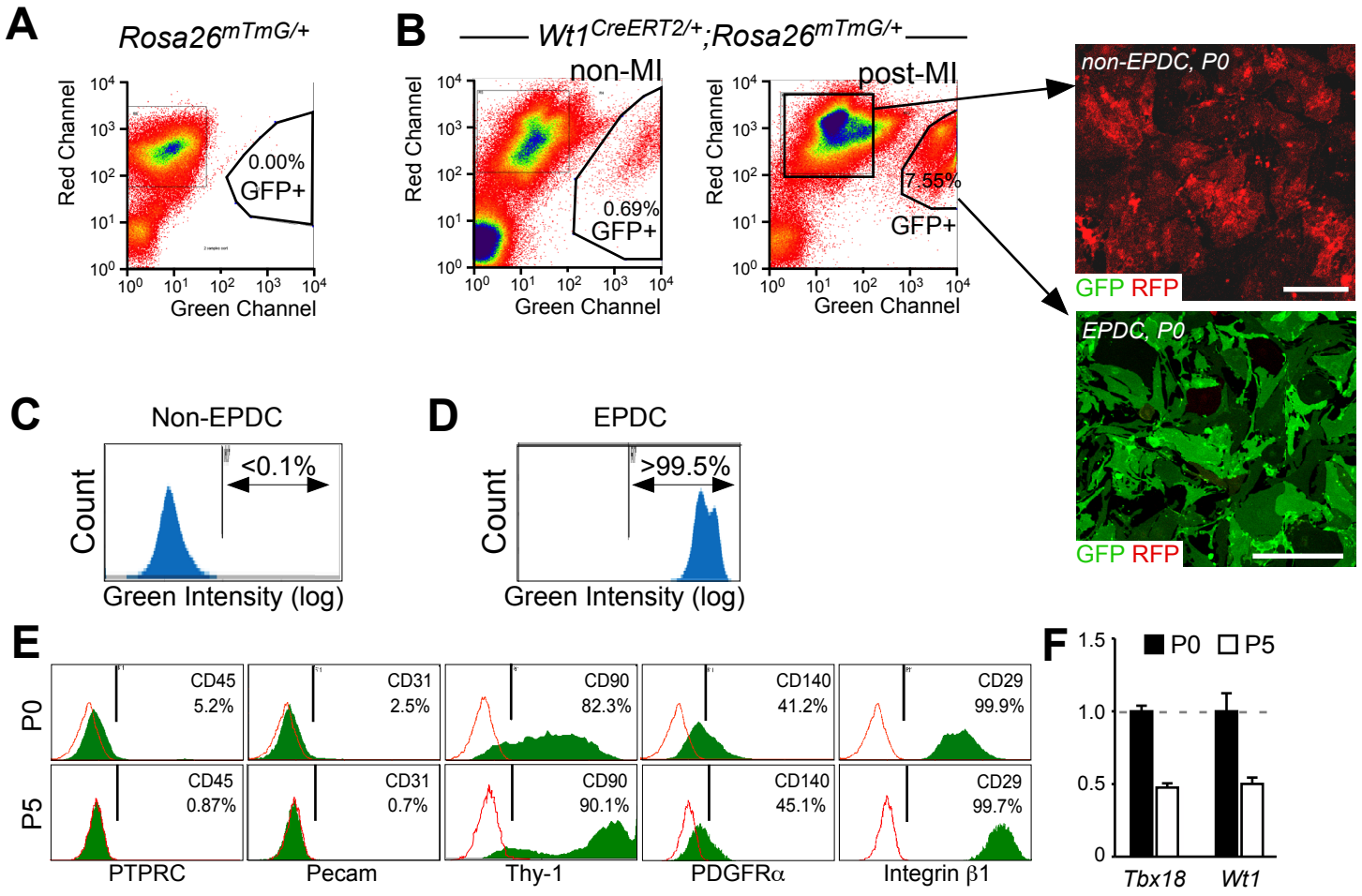

Supplemental Figure 9

Isolation and amplification of EPDCs. (**A**) FACS sorting negative control. There was no GFP signal in *Rosa26*$^{mTmG/+}$ hearts (0.00%). (**B**) GFP^{+} cells were sorted from non-MI and post-MI *Wt1*$^{CreERT2/+}$;*Rosa26*$^{mTmG/+}$ hearts. EPDCs increased after MI. Sorted cells were placed in culture and imaged to verify the purity of sorted populations. Note lack of GFP^{+} cells in the non-EPDC population, and lack of RFP^{+} cells in the EPDC population. In the FACS plots, there was signal in the red channel with strong GFP fluorescence because of spillage of GFP emission into the red channel. This can be controlled for using the negative control sample to properly set the FACS gates. Bar = 50 μm. (**C, D**) P5 EPDCs were analyzed by FACS. Histograms indicate the fraction of GFP+ cells. EPDCs retained their purity after 5 passages. (**E**) FACS analysis of surface marker profile of primary (P0) and P5 EPDCs. Surface marker profile was stable over 5 passages. Red lines indicate isotype-matched IgG, and green areas indicate signal with specific antibody. (**F**) Expression of epicardial marker genes *Tbx18* and *Wt1* showed small but statistically significant changes over 5 passages. n = 3-4.

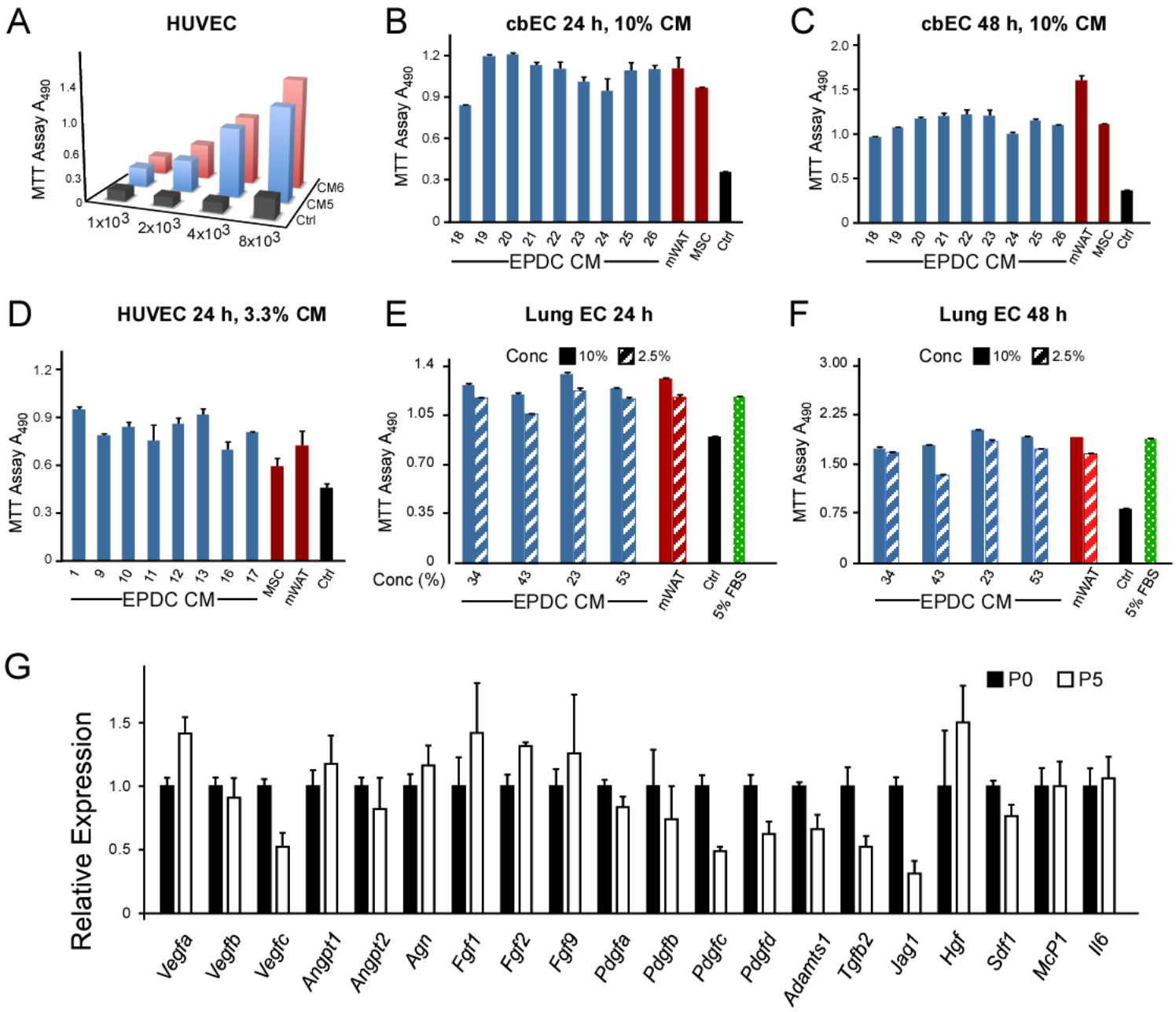

Supplemental Figure 10

Proangiogenic effect of EPDC conditioned media. (**A-F**) EPDC CM stimulated expansion of endothelial cells. CM from EPDCs derived from separate mice were tested separately, and designated "CM" followed by a number. CM43 was derived from embryo EPDC, while other CM was from adult EPDC. EPDC CM (blue columns) significantly increased the proliferation of cells compared with unconditioned medium (Ctrl, black columns). The effect of EPDC CM was comparable to that of positive control media conditioned by MSCs and mouse white adipocyte tissue derived mesenchymal stromal cells (mWAT; red columns). This was true at a range of starting cell numbers. Each bar is the average of 3 repeats. (**G**) Angiogenesis genes comparison between P0 and P5 EPDCs. n=3-4.

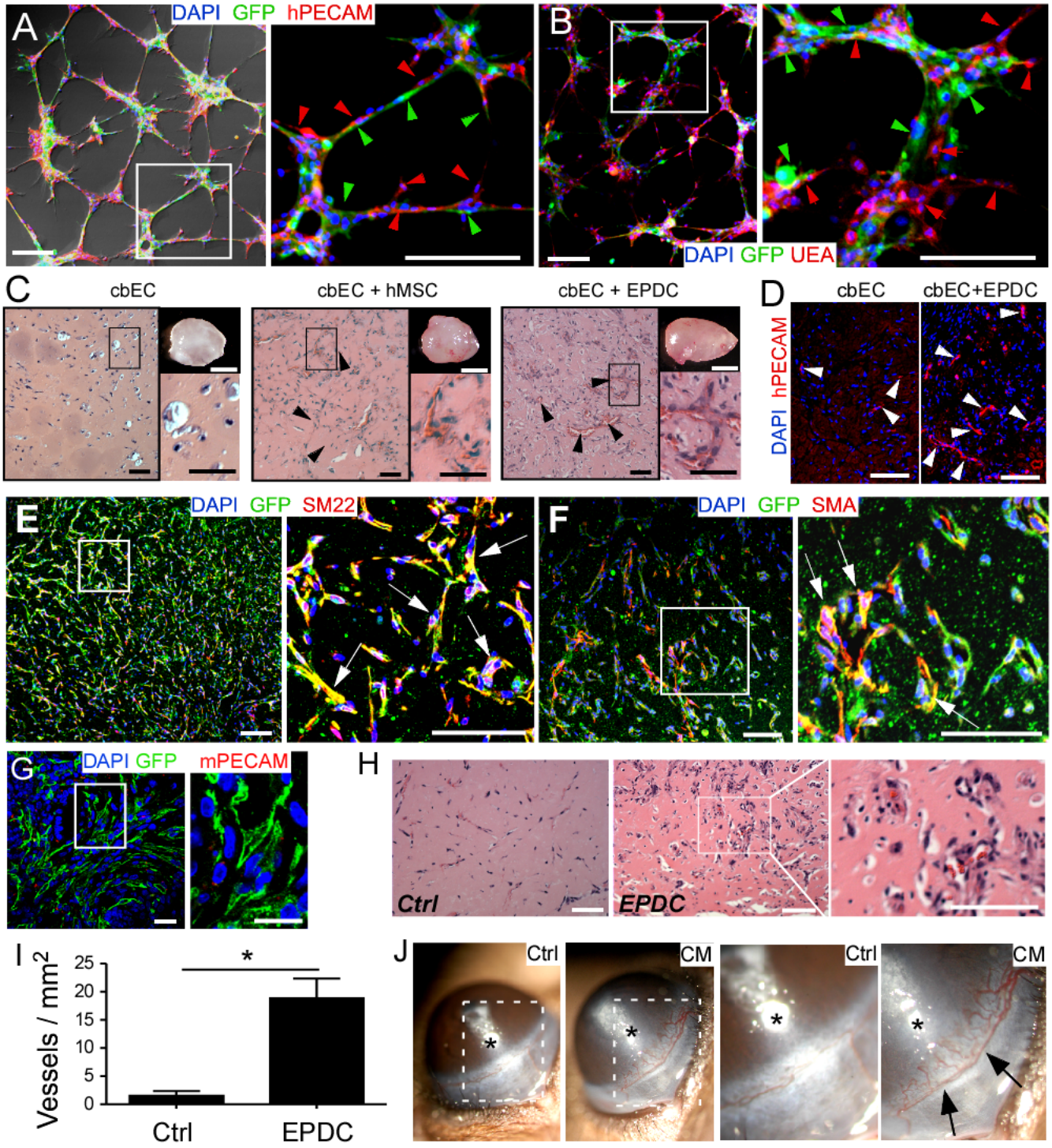

Supplemental Figure 11

EPDCs promote angiogenesis. (**A,B**) In EPDC (green arrowheads) and HUVEC (red arrowheads) cocultures, EPDC incorporated into and promoted vessel-like tube formation. HUVEC were stained with human PECAM antibody or UEA, which labels human ECs. EPDCs were marked with GFP. Bar = 200 μm. (**C-G)** Matrigel plug assay using cbECs with or without EPDCs. (**C**). Gross appearance and H.E. stained sections of plugs. cbECs alone yielded pale plugs with few blood-filled vessels (arrowheads), while addition of EPDCs or MSCs yielded pink, relatively better vascularized plugs with more blood-filled vessels. White bar = 2mm; black bar = 50 μm. (**D**) EPDC-containing matrigel plugs had more PECAM$^+$ vessels (arrowheads). Bar = 100 μm. (**E, F**) GFP$^+$ EDPCs expressed pericytes and smooth muscle cell markers SM22 and SMA (white arrows). Bar = 100 μm. (**G**) GFP-marked EPDCs did not adopt endothelial cell fate (red, mouse PECAM antibody). Bar = 20 μm. (**H-I**) Matrigel plugs without cells or with EPDCs alone. In these plugs lacking cbECs, 1 week after implantation EPDCs recruited host endothelial cells to form blood-filled vessels. H.E. staining showed greater blood-filled vessels in matrigel plugs containing EPDCs compared to plugs without cells (Ctrl). Bar = 100 μm. (**I**) Quantification of blood-filled vessels in showed greater density with EPDCs. *$P < 0.05$, n=4. (**J**) Implantation of pellets (asterisk) loaded with concentrated EPDC conditioned media (CM) stimulated corneal angiogenesis. Pellets loaded with unconditioned media (Ctrl) did not stimulate angiogenesis. Right images are magnifications of boxed areas.

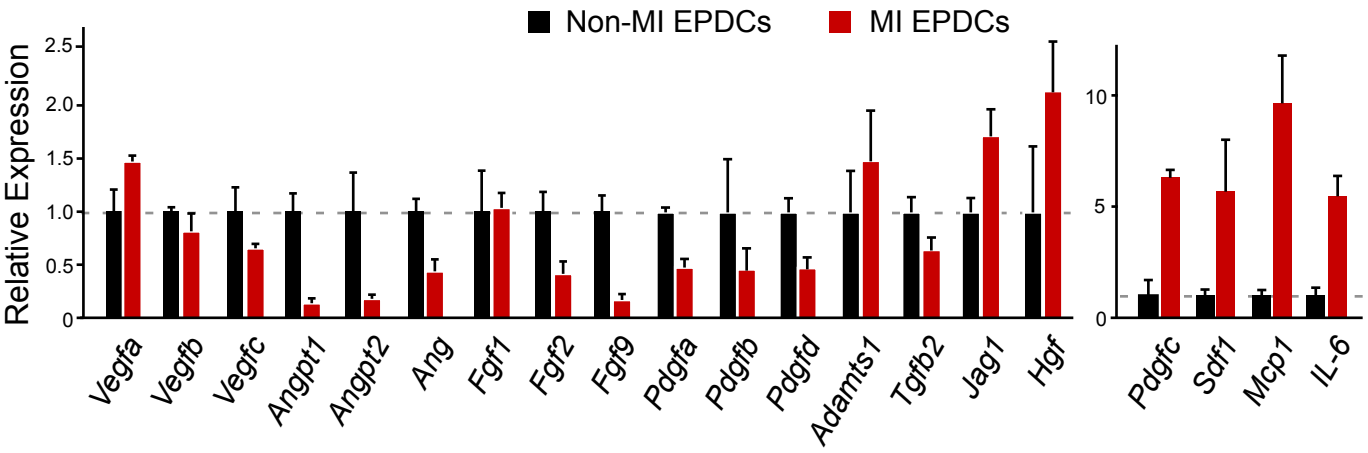

Supplemental Figure 12
Expression of angiogenesis genes in non-MI EPDCs and MI EPDCs. Expression was compared by qRTPCR. n=3-4. MI altered expression of some genes and did not appear to uniformly activate pro-angiogenic gene expression between the small fraction of epicardial cells labeled by $Wt1^{CreERT2}$ in normal adult epicardium (non-MI EPDCs) and post-MI EPDCs of the expanded epicardial layer.

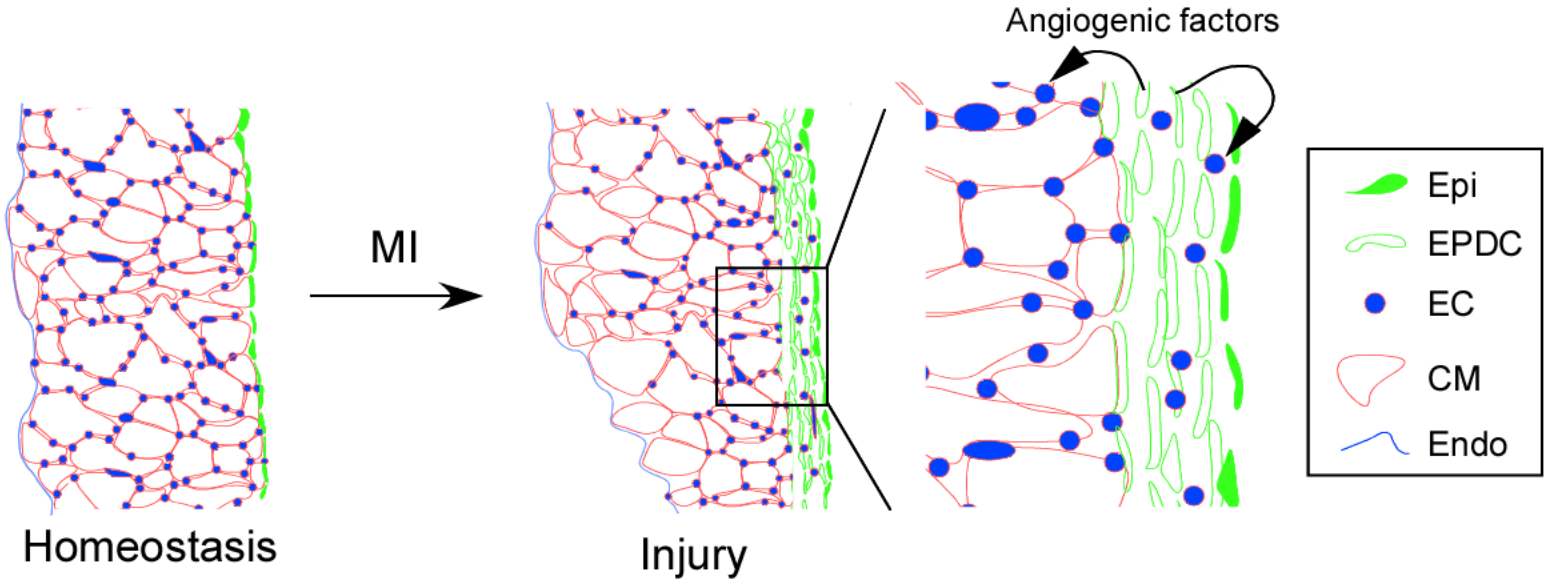

Supplemental Figure 13
Adult epicardium modulates myocardial injury by secretion of paracrine factors. The epicardium is a thin, quiescent sheet in the normal adult heart. Myocardial infarction reactivates a fetal epicardial program including epicardial proliferation, fetal gene expression, and epithelial to mesenchymal transition to form mesenchymal EPDCs. The epicardium thickens with EPDCs, which secrete angiogenic factors that promote angiogenesis after MI.

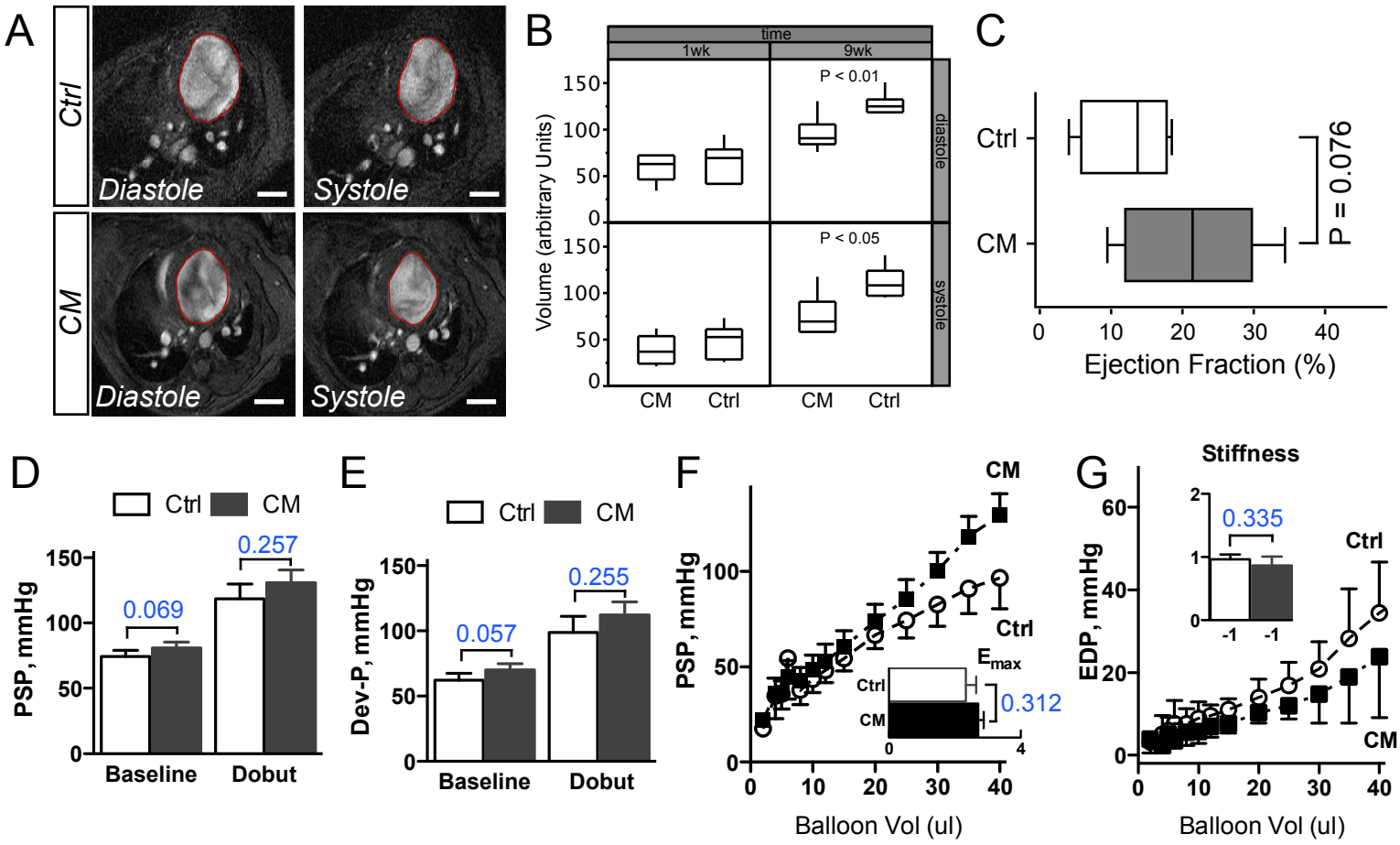

Supplemental Figure 14

Long term effect of CM treatment on heart function. (**A**) Cine-MR images obtained 9 weeks post MI. Red line indicates the left ventricular chamber area. (**B**) LV volume in systole and diastole, measured by MRI. There was significantly less adverse LV remodeling in CM-treated hearts at 9 weeks ($P < 0.05$; $n = 6$). (**C**) Ejections fraction, calculated from five stacked slices, was compared between CM injected heats and Control groups. Although the ejection fraction was not significantly higher in CM compared to control treatment ($P = 0.076$), the CM-treated hearts have a improved trend in function ($n = 6$). (**D-G**) Measure of LV systolic and diastolic function were not significantly different in CM treated hearts 9 weeks post MI. Peak and developed systolic pressure (PSP and Dev-P) and E_{max}, measures of systolic function were higher, but did not reach statistical significance at baseline and with dobutamine stress. Left ventricular stiffness was also not significantly different with CM at this time point. Numbers in blue indicate p-values ($n = 6 - 7$).